Synthesis and Characterization of Some Mixed Alkyl Thiocarbamates of Gallium and Indium, Precursors for III/VI Materials: The X-ray Single-Crystal Structures of Dimethyl- and Diethylindium Diethyldithiocarbamates

S. W. Haggata, M. Azad Malik, M. Motevalli, and P. O'Brien*

Department of Chemistry, Queen Mary & Westfield College, Mile End Road, London E1 4NS, U.K.

J. C. Knowles

I.R.C., Biomedical Materials, Queen Mary and Westfield College, Mile End Road, London E1 4NS, U.K.

Received November 1, 1994. Revised Manuscript Received February 9, 1995[⊗]

A series of mixed alkyl/dithiocarbamates of the general formula $R_2MS_2CNEt_2$ (M = In or Ga and R = Me, Et, or neopentyl) have been prepared and characterized. The indium complexes are well-defined crystalline solids, and X-ray single-crystal structures are reported for the methyl and ethyl compounds. Both compounds have S_2C_2 coordination at indium, and all bond lengths and angles are in the normal range. The gallium complexes are all liquids. The indium compounds have been used to successfully deposit thin films of various phases of In_xS_y by low-pressure MOCVD onto GaAs(100) substrates. The methyl complex deposits orthorhombic InS[39] and monoclinic In_6S_7[39] phases between 425 and 400 °C; growth at 325 °C resulted in the cubic β-In_2S_3 phase. In contrast the ethyl compound deposits monophasic β-In_2S_3 over the 400-350 °C, the neopentyl indium compound deposits In_6S_7 at 400 and 375 °C with the presence of a small amount of the β-In_2S_3. Preliminary results of deposition experiments with the gallium precursors were less successful, and only very thin films were grown.

Introduction

A considerable amount of work has been published on the synthesis of single-molecule precursors for the deposition of III/V[1-3] or II/VI[4-8] semiconducting materials; however, only a handful of reports are available on the preparation of III/VI materials from such precursors.[9-18] Thin films of In_xS_x or Ga_xS_x have electrical, optical, and photovoltaic properties suitable for use in various optoelectronic devices.[19] Such materials may be classified as midbandgap semiconductors, e.g., InS[12] (2.44 eV)[20] and β-In_2S_3[11,14] (2.07 eV)[21] as compared to materials such as GaAs[22] (narrow bandgap, 1.42 eV) and ZnS[22] (wide bandgap, 3.68 eV). Such sulfur-containing materials may be useful in passivating the surface of III/V compounds.[23] Single-molecule precursors for the deposition of III/VI materials recently prepared include $Me_2InSePh$,[9] $In(SePh)_3$,[9] $^nBuIn(S\text{-}i\text{-}Pr)_2$,[11,12] and $[In_2Se_{21}]$.[13] Solution pyrolysis of the precursors $^iBu_2InS\text{-}n\text{-}Pr$[12] and $Cu(S_2CN^nBu_2)_2$[24,17] affords the related ternary chalcopyrite $CuInS_2$[17] which is an important solar-cell material. It has been suggested[10,16] that the structure of such precursors may determine the phase of a film deposited; particularly elegant examples include the decomposition of the cubane $[(^tBu)GaS]_4$[10] and dimeric

* To whom correspondence should be addressed at Department of Chemistry, Imperial College of Science Technology and Medicine, London, SW7 2AZ U.K.

⊗ Abstract published in *Advance ACS Abstracts,* March 15, 1995.

(1) Cowley, A. H.; Jones, R. A. *Angew. Chem., Int. Ed. Engl.* **1989**, *28*, 1208.
(2) Arif, A. M.; Benac, B. L.; Cowley, A. H.; Jones, R. A.; Kidd, K. B.; Nunn, C. M. *J. Chem. Soc.* **1988**, *12*, 553.
(3) Aitchison, K. A.; Julius Backer-Dirks, J. D.; Bradley, D. C.; Faktor, M. M.; Frigo, D. M.; Hursthouse, M. B.; Hussain, B.; Short, R. L. *J. Organomet. Chem.* **1989**, *366*, 11.
(4) Malik, M. A.; O'Brien, P. *Mater. Chem.* **1991**, *3*, 999.
(5) Malik, M. A.; O'Brien, P.; Hursthouse, M. B.; Motevalli, M. *Organometallics* **1991**, *10*, 730.
(6) Malik, M. A.; O'Brien, P.; Hursthouse, M. B.; Motevalli, M. *Polyhedron* **1992**, *11*, 45.
(7) Malik, M. A.; O'Brien, P.; Hursthouse, M. B.; Motevalli, M. *J. Mater. Chem.* **1992**, *2*, 949.
(8) Malik, M. A.; O'Brien, P.; Hursthouse, M. B.; Motevalli, M. *Organometallics* **1992**, *11*, 3136.
(9) Gysling, H. J.; Wernberg, A. A.; Blanton, T. N. *Chem. Mater.* **1992**, *4*, 900.
(10) (a) MacInnes, A. N.; Power, M. B.; Barron, A. R. *Chem. Mater.* **1992**, *4*, 11; *Ibid.* **1993**, *5*, 1344.
(11) Nomura, R.; Konishi, K.; Matsuda, H. *Thin Solid Films* **1991**, *198*, 339.
(12) Nomura, R.; Fujii, S.; Kanaya, K.; Matsuda, H. *Polyhedron* **1990**, *9*, 361.
(13) Kanatzidis, M. G.; Dihingra, S. *Inorg. Chem.* **1989**, *28*, 2024.
(14) Kim, Wha-Tek; Kim, Chang-Dae; *J. Appl. Phys.* **1986**, *60*, 2631.
(15) Nomura, R.; Moritake, A.; Kanaya, K.; Matsuda, H. *Thin Solid Films* **1988**, *167*, L27-L29.
(16) MacInnes, A. N.; Cleaver, W. M.; Barron, A. R.; Power, M. B.; Hepp, A. F. *Adv. Mat. Opt. Electron.* **1992**, *1*, 229.
(17) Nomura, R.; Kanaya, K.; Matsuda, H. *Chem. Lett.* **1988**, 1849-1850.
(18) Nomura, R.; Inazawa, S.; Kanaya, K.; Matsuda, H. *Polyhedron* **1989**, *8*, 763.
(19) Sze, S. M. *Semiconductor Devices, Physics and Technology*; John Wiley and Sons: Chichester, 1985.
(20) Nishino, T.; Hamakawa, Y. *Jpn. J. Appl. Phys.* **1977**, *16*, 1291.
(21) Becker, R. S.; Zheng, T.; Elton, J.; Saeki, M. *Sol. Energy Mater.* **1986**, *13*, 97.
(22) O'Brien, P. *Inorganic Materials*; Bruce, D. W., O'Hare, D., Eds.; John Wiley and Sons: Chichester, 1992; Chapter 9, p 491.
(23) (a) MacInnes, A. N.; Power, M. B.; Barron, A. R.; Jenkins, P. P.; Hepp, A. F. *Appl. Phys. Lett.* **1993**, *62*, 711. (b) Tabib-Azar, M.; Kang, S.; MacInnes, A. N.; Power, M. B.; Barron, A. R.; Jenkins, P. P.; Hepp, A. F. *Appl. Phys. Lett.* **1993**, *63*, 625.23.
(24) Nomura, R.; Takabe, A.; Matsuda, H. *Polyhedron* **1987**, *6*, 411.

0897-4756/95/2807-0716$09.00/0

Table 1. Elemental Analyses of Compounds 1–6

mol formula	emp formula	found % (calcd %) C	H	N
$(CH_3)_2InS_2CN(C_2H_5)_2$ (**1**)	$C_7H_{16}NS_2In$	28.61 (28.68)	5.44 (5.50)	4.80 (4.77)
$(C_2H_5)_2InS_2CN(C_2H_5)_2$ (**2**)	$C_9H_{20}NS_2In$	33.41 (33.65)	6.32 (6.27)	3.96 (4.36)
$(C_5H_{11})_2InS_2CN(C_2H_5)_2$ (**3**)	$C_{15}H_{32}NS_2In$	42.99 (44.40)	7.97 (7.96)	3.30 (3.45)
$(CH_3)_2GaS_2CN(C_2H_5)_2$ (**4**)	$C_7H_{16}NS_2Ga$	34.30 (33.89)	5.91 (6.50)	5.44 (5.65)
$(C_2H_5)_2GaS_2CN(C_2H_5)_2$ (**5**)	$C_9H_{20}NS_2Ga$	38.70 (39.15)	7.26 (7.30)	4.84 (5.07)
$(C_5H_{11})_2GaS_2CN(C_2H_5)_2$ (**6**)	$C_{15}H_{32}NS_2Ga$	49.65 (50.00)	8.87 (8.95)	3.47 (3.89)

Table 2. Crystal Data and Structure Refinement

	1	**2**
empirical formula	$C_7H_{16}InNS_2$	$C_9H_{20}InNS_2$
formula weight	293.15	321.20
temp	293(2) K	293(2) K
wavelength	0.71069 Å	0.71069 Å
crystal system	triclinic	monoclinic
space group	$P\bar{1}$	$P21/c$
unit-cell dimensions	a = 9.841(1) Å b = 9.894(1) Å c = 14.300(2) Å α = 90.241(1)° β = 73.600(1)° γ = 116.800(1)°	a = 9.975(3) Å b = 14.667(4) Å c = 9.931(8) Å α = 90° β = 98.81(5)° γ = 90°
volume	1179.8(2) Å^3	1435.8(13) Å^3
Z	4	4
density (calculated)	1.650 mg/m^3	1.486 mg/m^3
absorption coefficient	2.307 mm^{-1}	1.903 mm^{-1}
$F(000)$	584	648
θ range for data collection	1.50–24.97°	2.07–24.98°
index ranges	$-11 \le h \le 10, 0 \le k \le 11, -16 \le l \le 16$	$0 \le h \le 11, -7 \le k \le 17, -11 \le l \le 11$
reflections collected	4511	2724
independent reflections	4136 [R(int) = 0.0093]	2513 [R(int) = 0.0203]
refinement method	full-matrix least-squares on F^2	full-matrix least-squares on F^2
data/restraints/parameters	4136/0/220	2508/0/131
goodness-to-fit on F^2	0.834	0.864
final R indexes [$I > 2\sigma(I)$]	$R1$ = 0.0251 $wR2$ = 0.0829	$R1$ = 0.0813 $wR2$ = 0.2332
R indexes (all data)	$R1$ = 0.0362 $wR2$ = 0.0870	$R1$ = 0.1807 $wR2$ = 0.2834
largest diff peak and hole	0.450 and −0.496 (eÅ^{-3})	0.863 and −0.721 (eÅ^{-3})

$[(^tBu)_2In(S^tBu)]_2$[16] to yield a cubic phases of GaS and tetragonal InS, respectively.

In a series of papers we have developed the chemistry of mixed alkyl/dithio or diseleno carbamates of group 12 metals and demonstrated that these compounds can be used as precursors for the deposition of II/VI materials. Although Maeda et al.[25] have reported the synthesis of several simple indium and gallium dithiocarbamates, the chemistry of any mixed compounds formed with alkyls has not been investigated for the group III metals. In this paper, we report the synthesis of several new dithiocarbamates of gallium and indium. Deposition studies are reported for a series of precursors of the general formula $[R_2MS_2CNEt_2]$ (M = Ga, In; R = Me, Et, Np). All the new compounds have been characterized by a range of various spectroscopic techniques. The structures of $[Me_2InS_2CNEt_2]$ (**1**) and $[Et_2InS_2CNEt_2]$ (**2**) have been determined by single-crystal X-ray diffraction methods.

Experimental Section

Chemicals. Bromoethane, 1-bromo-2,2-dimethylpropane, sodium diethyldithiocarbamate, gallium(III) chloride, indium(III) chloride, and magnesium turnings were purchased from Aldrich Chemical Co. Ltd. Trimethylgallium and trimethylindium were kindly donated by Epichem Ltd. Solvents were obtained from BDH and were dried and degassed before use. The compounds $ClEt_2In$,[26] $ClNp_2In$,[27] $ClEt_2Ga$,[28] $ClNp_2Ga$,[29] $In(S_2CNEt_2)_3$,[30] and $Ga(S_2CNEt_2)_3$[30] were prepared by the literature methods.

Synthesis. All reactions were performed in an inert atmosphere using Schlenk techniques and a vacuum line.

Preparation of $Me_2InS_2CNEt_2$ (1). (a) In an attempt to prepare a mixed-metal alkyl dithiocarbamate complex of indium and zinc, bis(diethyldithiocarbamato)zinc(II) (5.4 g, 14.9 mmol) was reacted with trimethylindium (2.4 g, 14.9 mmol) in toluene. The mixture was stirred and heated at 70 °C for 0.5 h. On cooling, white cubic crystals settled out which were separated by decanting the solvent into another flask. The product was identified as methyldiethyldithiocarbamatozinc(II)[4] by its NMR and mp (140 °C). The decanted solvent, on concentration, gave a second crop of large transparent crystals with a substantially different melting point (84 °C). The compound was identified as dimethyldiethyldithiocarbamatoindium(III) (**1**).

(b) The same compound was also prepared by a comproportionation reaction between stoichiometric amounts of tris(diethyldithiocarbamato)indium(III)[30] (5.7 g, 10.2 mmol) and trimethylindium (3.3 g, 20.4 mmol) in toluene (40 mL). The mixture was stirred at room temperature for half an hour and then heated to 50 °C and stirred for further 10 min. On concentration, white crystals settled out from the clear solution (7.90 g, 88%), mp 84 °C.

(25) Maeda, T.; Okawara, R. *J. Organomet. Chem.* **1972**, *39*, 87.
(26) Yasuda, K.; Okawara, R. *Inorg. Nucl. Chem. Lett.* **1967**, *3*, 135.
(27) Beachley, O. T. Jr.; Spiegel, E. F.; Kopaz, J. P.; Rogers, R. D. *Organometallics* **1989**, *8*, 1915.
(28) Eisch, J. J. *J. Am. Chem. Soc.* **1962**, *84*, 3830.
(29) Beachley, O. T. Jr.; Pazik, J. C. *Organometallics* **1988**, *7*, 1516.
(30) Dymock, K.; Palenik, G. J.; Slezak, J.; Raston, C. L.; White, A. H. *J. Chem. Soc., Dalton Trans.* **1976**, 28.

Table 3. Atomic Coordinates ($\times 10^4$) and Equivalent Isotropic Displacement Parameters ($Å^2 \times 10^3$)[a]

	x	*y*	*z*	*U*(eq)
		Compound **1**		
In(1)	347(1)	5550(1)	2986(1)	55(1)
In(2)	−203(1)	10275(1)	2006(1)	56(1)
S(1)	−1480(1)	2803(1)	2568(1)	54(1)
S(2)	−660(1)	5804(1)	1561(1)	63(1)
S(3)	1643(1)	9199(1)	2414(1)	51(1)
S(4)	817(1)	11466(1)	3427(1)	60(1)
N(1)	−2685(4)	3165(4)	1183(2)	54(1)
N(2)	2760(4)	10566(4)	3847(2)	51(1)
C(1)	2755(5)	5913(6)	2443(4)	78(1)
C(2)	−1209(5)	5702(5)	4321(3)	73(1)
C(3)	−1710(4)	3840(4)	1711(2)	46(1)
C(4)	−3006(5)	4056(6)	541(3)	71(1)
C(5)	−4337(6)	4399(7)	1100(4)	100(2)
C(6)	−3637(5)	1484(5)	1283(3)	68(1)
C(7)	−3040(7)	844(6)	415(4)	96(2)
C(8)	1838(4)	10410(4)	3296(2)	45(1)
C(9)	1307(6)	11786(6)	663(3)	81(1)
C(10)	−2622(5)	8489(5)	2564(4)	74(1)
C(11)	3019(5)	11685(5)	4542(3)	69(1)
C(12)	4364(6)	13217(6)	4060(4)	96(2)
C(13)	3688(4)	9730(4)	3763(3)	56(1)
C(14)	3013(5)	8501(6)	4630(3)	83(1)
		Compound **2**		
In	7532(1)	4451(1)	218(1)	123(1)
S(1)	6056(3)	5922(2)	40(4)	125(1)
S(2)	8941(3)	5874(3)	−130(5)	174(2)
N(1)	7466(9)	7367(7)	−439(13)	151(4)
C(1)	7472(9)	6463(8)	−159(10)	105(3)
C(2)	6193(12)	7914(9)	−617(14)	135(4)
C(3)	6021(17)	8279(10)	745(17)	221(8)
C(4)	8846(14)	7940(10)	−397(19)	235(8)
C(5)	9136(23)	7906(15)	−1463(23)	324(15)
C(6)	7242(18)	3656(10)	−1617(20)	215(8)
C(7)	7432(14)	4318(9)	−2659(15)	159(6)
C(8)	7881(21)	4033(10)	2393(22)	258(11)
C(9)	7525(16)	4468(9)	3553(23)	209(8)

[a] *U*(eq) is defined as one-third of the trace of the orthogonalized U_{ij} tensor.

Preparation of $Et_2InS_2CNEt_2$ (2), $Np_2InS_2CNEt_2$ (3), $Et_2GaS_2CNEt_2$ (5), and $Np_2GaS_2CNEt_2$ (6). In a typical preparation of **2**, sodium diethyldithiocarbamate (2.73 g, 15.97 mmol) was added to a solution of chlorodiethylindium[26] (3.33 g, 15.97 mmol) in ether (60 mL) and stirred for 12 h at room temperature. A white solid (NaCl) formed during the reaction which was removed by filtration. The colorless filtrate containing the product was evaporated to dryness under vacuum. The solid product contained traces of salt and was dissolved in petroleum spirits (60−80 °C) and filtered. The filtrate, on concentration, gave white crystals of diethyldiethyldithiocarbamatoindium(III) (3.33 g, 65%), mp 57 °C. Compound **3** was obtained as a white crystalline solid (2.97 g, 70%), mp 44 °C. Compounds **5** (4.51 g, 75%) and **6** (3.25 g, 72%), both liquids, were prepared in a similar manner.

Preparation of $Me_2GaS_2CNEt_2$ (4). Compound **4**, a liquid, was prepared by the addition of tris(diethyldithiocarbamato)-gallium(III)[30] (4.37 g, 8.48 mmol) to a stirred solution of trimethylgallium (1.96 g, 16.97 mmol) which was dissolved in toluene (60 mL). The trisdithiocarbamate dissolved immediately. The colorless solution was stirred overnight. The solvent and any volatiles were then removed in vacuo giving a colorless liquid, dimethyldiethyldithiocarbamatogallium(III) (4.3 g, 67%). All compounds had satisfactory microanalysis (Table 1).

Main Spectroscopic Properties. [$Me_2InS_2CNEt_2$] (**1**): Major IR bands (cm^{-1}) 374 (νIn−S); 520, 565 (νIn−C), 984 (νC−S), 1494 (νC−N). ^1H NMR δ (C_6D_6, 25 °C, 250 MHz) 0.34 [6H, s, In(CH_3)$_2$], 0.88 [6H, t, $^3J_{H-H}$ 7.1 Hz, (CH_3CH_2)$_2$N], 3.35 [4H, q, $^3J_{H-H}$ 7.1 Hz, (CH_3CH_2)$_2$N]. ^{13}C NMR δ (C_6D_6, 25 °C, 250 MHz) 201.92 [−CS_2−], −3.24 [Ga(CH_3)$_2$], 47.79 [(CH_3-CH_2)$_2$N], 11.62 [(CH_3CH_2)$_2$N]. Mass spectrum (*m*/*z*) $(CH_3)In^+S_2CNEt_2$ 278 (100.0%), $(CH_3)_2In^+$ 145 (0.4%), SC^+NEt_2 116 (66.1%), ^{115}In 115 (91.1%), $SC^+NEt(H)$ 88 (17.3%), SC^+NEt 87 (2.7%), $(EtN)_2$ 86 (33.3%), N^+Et_2 72 (4.6%), $N^+Et(H)$ 44 (16.05%).

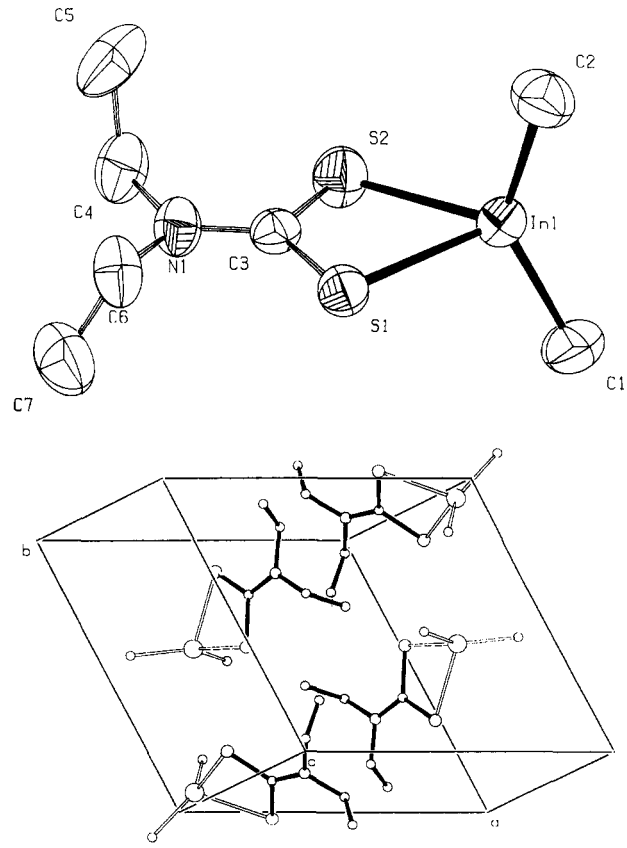

Figure 1. (a) X-ray structure of dimethyldiethyldithiocarbamatoindium(III). (b) Packing diagram for dimethyldiethyldithiocarbamatoindium(III).

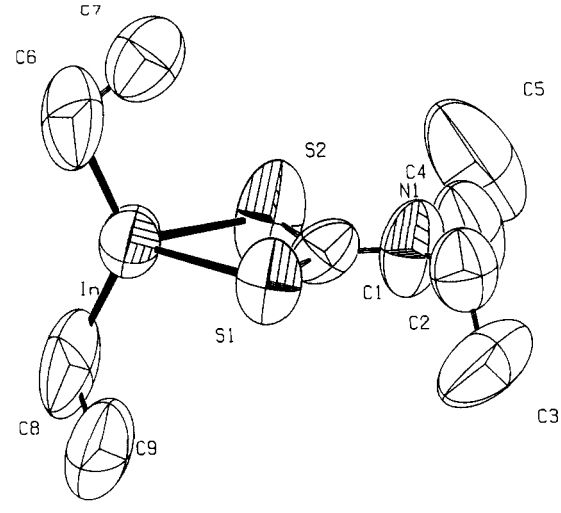

Figure 2. X-ray structure of diethyldiethyldithiocarbamatoindium(III).

[$Et_2InS_2CNEt_2$] (**2**): Major IR bands (cm^{-1}) 375 (νIn−S); 498, 561 (νIn−C), 1008 (νC−S), 1494 (νC−N). ^1H NMR δ (C_6D_6, 25 °C, 250 MHz) 1.04 [4H, q, $^3J_{H-H}$ 8.25 Hz, In-(CH_2CH_3)$_2$], 1.63 [6H, t, $^3J_{H-H}$ 8.25 Hz, In(CH_2CH_3)$_2$], 3.39 [4H, q, $^3J_{H-H}$ 7.1 Hz, (CH_3CH_2)$_2$N], 0.81 [6H, t, $^3J_{H-H}$ 7.1 Hz, (CH_3CH_2)$_2$N]. ^{13}C NMR δ (C_6D_6, 25 °C, 250 MHz) 203.17 [−CS_2−], 10.77 [In(CH_2CH_3)$_2$], 13.04 [In(CH_2CH_3)$_2$], 48.56 [(CH_3CH_2)$_2$N], 12.52 [(CH_3CH_2)$_2$N]. Mass spectrum (*m*/*z*) C_2H_5-$In^+S_2CNEt_2$ 292 (100.0%), $In^+S_2CNEt_2$ 263 (16.2%), HIn^+Et 145 (3.3%), SC^+NEt_2 116 (26.4%), ^{115}In 115 (89.8%), SC^+NEt-(H) 88 (16.5%), $(EtN)_2$ 86 (22.6%), $^+NEt_2$ 72 (9.3%), SCN 58 (21.0%), $N^+Et(H)$ 44 (15.0%).

[$Np_2InS_2CNEt_2$] (**3**): Major IR bands (cm^{-1}) 379 (νIn−S); 567, 589 (νIn−C), 1001 (νC−S), 1492 (νC−N). ^1H NMR δ

Table 4. Selected Bond Lengths (Å) and Angles (deg)

	1	2
In−C(1), C(6)	2.13(4)	2.15(2)
In−C(2), C(8)	2.14(4)	2.22(2)
In−S(2)	2.56(10)	2.57(4)
In−S(1)	2.68(10)	2.60(3)
S(1)−C(1), C(3)	1.73(3)	1.66(10)
S(2)−C(1), C(3)	1.72(3)	1.70(10)
C(1), C(6)−In−C(2), C(8)	137.5(2)	131.1(6)
C(1), C(6)−In−S(2)	110.72	109.4(4)
C(2), C(8)−In−S(2)	108.6(13)	110.4(5)
C(1), C(6)−In−S(1)	106.2(13)	113.0(5)
C(2), C(8)−In−S(1)	102.5(12)	107.3(4)
S(2)−In−S(1)	68.8(3)	68.5(10)
C(3), C(1)−S(1)−In	84.5(11)	85.5(4)
C(3), C(1)−S(2)−In	88.2(12)	85.8(4)
S(2)−C(3), C(1)−S(2)	118.3(2)	120.2(7)

(C_6D_6, 25 °C, 250 MHz), 1.48 [4H, s, In($CH_2C(CH_3)_3)_2$], 1.29 [18H, s, In($CH_2C(CH_3)_3)_2$], 3.36 [4H, q, $^3J_{H-H}$ 7.1 Hz, ($CH_3CH_2)_2N$], 0.90 [6H, t, $^3J_{H-H}$ 7.1 Hz, ($CH_3CH_2)_2N$]. ^{13}C NMR δ (C_6D_6, 25 °C, 250 MHz) 202.17 [$-CS_2-$], 41.59 [In($CH_2C(CH_3)_3)_2$], 33.49 [In($CH_2C(CH_3)_3)_2$], 35.34 [In($CH_2C(CH_3)_3)_2$], 48.47 [($CH_3CH_2)_2N$], 12.56 [($CH_3CH_2)_2N$]. Mass spectrum (*m/z*) $(C_5H_{11})In^+S_2CNEt_2$ 334 (100.0%), $(C_5H_{11})_2In^+$ 237 (0.8%), SC^+NEt_2 116 (16.0%), $SC^+NEt(H)$ 88 (3.9%), SC^+NEt 87 (1.0%), $(EtN)_2$ 86 (4.8%), $^+Et_2$ 72 (0.2%), N^+Et 43 (11.1%).

[$Me_2GaS_2CNEt_2$] (**4**): Major IR bands (cm^{-1}) 380 (νGa−S); 538, 584 (νGa−C), 1000 (νC−S), 1504 (νC−N). ^1H NMR δ (C_6D_6, 25 °C, 250 MHz), 0.32 [6H, s, Ga($CH_3)_2$], 3.21 [4H, q, $^3J_{H-H}$ 7.1 Hz, ($CH_3CH_2)_2N$], 0.80 [6H, t, $^3H_{H-H}$ 7.1 Hz, ($CH_3CH_2)_2N$]. ^{13}C NMR δ (C_6D_6, 25 °C, 250 MHz) 200.0 [$-CS_2-$], −0.86 [Ga($CH_3)_2$], 47.94 [($CH_3CH_2)_2N$], 12.44 [($CH_3CH_2)_2N$]. Mass spectrum (*m/z*): $^{71}(CH_3)_2Ga^+S_2CNEt_2$ 234 (100.0%), $^{71}(CH_3)Ga^+S_2CNEt_2$ 219 (0.7%), $^{69}(CH_3)Ga^+S_2CNEt_2$ 217 (1.1%), $^{71}Ga^+S_2C$ 147 (0.4%), $^{69}Ga^+S_2C$ 145 (0.6%), $^{71}(CH_3)_2Ga^+$ 101 (7.0%), $^{69}(CH_3)_2Ga^+$ 99 (12.0%), SC^+Net_2 116 (45.8%), $SC^+NEt(H)$ 88 (28.5%), SC^+NEt 87 (1.3%), NEt_2 86 (8.5%), N^+Et_2 72 (3.5%), $^{71}Ga^+$ 71 (18.0%), $^{69}Ga^+$ 69 (26.8%), $N^+Et(H)$ 44 (7.7%).

[$Et_2GaS_2CNEt_2$] (**5**): Major IR bands (cm^{-1}) 378 (νGa−S); 515, 558 (νGa−C), 1003 (νC−S), 1500 (νC−N). ^1H NMR δ (C_6D_6, 25 °C, 250 MHz) 1.00 [4H, q, $^3J_{H-H}$ 8.25 Hz, Ga($CH_2CH_3)_2$], 1.51 [6H, t, $^3J_{H-H}$ 8.25 Hz, Ga($CH_2CH_3)_2$], 3.26 [4H, q, $^3J_{H-H}$ 7.1 Hz, ($CH_3CH_2)_2N$], 0.83 [6H, t, $^3J_{H-H}$ 7.1 Hz, ($CH_3CH_2)_2N$]. ^{13}C NMR δ (C_6D_6, 25 °C, 250 MHz) 200.45 [$-CS_2-$], 8.54 [Ga($CH_2CH_3)_2$], 11.27 [Ga($CH_2CH_3)_2$], 47.94 [($CH_3CH_2)_2N$], 12.431 [($CH_3CH_2)_2N$]. Mass spectrum (*m/z*) $^{71}(C_2H_5)Ga^+S_2CNEt_2$ 248 (77.3%), $^{69}(C_2H_5)Ga^+S_2CNEt_2$ 246 (100.0%), $^{71}Ga^+S_2CNEt_2$ 219 (1.1%), $^{69}Ga^+S_2CNEt_2$ 217 (1.5%), $^{71}Ga^+S_2C$ 147 (0.4%), $^{69}Ga^+S_2C$ 145 (0.5%), $(C_2H_5)_2{}^{71}Ga^+$ 129 (2.3%), $(C_2H_5)_2{}^{69}Ga^+$ 127 (3.2%), SC^+NEt_2 116 (31.1%), $SC^+NEt(H)$ 88 (18.5%), SC^+NEt 87 (4.3%), N^+Et_2 72 (0.9%), $^{71}Ga^+$ 71 (8.5%), $^{69}Ga^+$ 69 (12.6%), $N^+Et(H)$ 44 (1.5%).

[$Np_2GaS_2CNEt_2$] (**6**): Major IR bands (cm^{-1}) 378 (νGa−S); 570, 595 (νGa−C), 1005 (νC−S), 1500 (νC−N). ^1H NMR δ (C_6D_6, 25 °C, 250 MHz), 1.20 [4H, s, Ga($CH_2C(CH_3)_3)_2$], 1.33 [18H, s, Ga($CH_2C(CH_3)_3)_2$], 3.24 [4H, q, $^3J_{H-H}$ 7.1 Hz, ($CH_3CH_2)_2N$], 0.83 [6H, t, $^3J_{H-H}$ 7.1 Hz, ($CH_3CH_2)_2N$]. ^{13}C NMR δ (C_6D_6, 25 °C, 250 MHz) 199.62 [$-CS_2-$], 38.83 [Ga($CH_2C(CH_3)_3)_2$], 33.17 [Ga($CH_2C(CH_3)_3)_2$], 34.81 [Ga($CH_2C(CH_3)_3)_2$], 47.80 [($CH_3CH_2)_2N$], 12.56 [($CH_3CH_2)_2N$]. Mass spectrum (*m/z*) $^{71}(C_5H_{11})Ga^+S_2CNEt_2$ 290 (73.5%), $^{69}(C_5H_{11})Ga^+S_2CNEt_2$ 288 (100.0%), $^{71}(C_5H_{11})_2Ga^+$ 213 (1.1%), $^{69}(C_5H_{11})_2Ga^+$ 211 (1.8%), $^{71}Ga^+S_2C$ 147 (2.0%), $^{69}Ga^+S_2C$ 145 (2.6%), $^{71}(C_5H_{11})Ga^+$ 142 (0.3%), $^{69}(C_5H_{11})_2Ga^+$ 140 (0.4%), SC^+NEt_2 116 (14.6%), $(EtN)_2$ 86 (2.3%), $SC^+NEt(H)$ 88 (9.0%), SC^+NEt 87 (1.9%), N^+Et_2 72 (0.9%), $^{71}Ga^+$ 71 (3.0%), $^{69}Ga^+$ 69 (4.0%), $N^+Et(H)$ 44 (1.9%), N^+Et 43 (5.7%).

Physical Measurements. NMR spectra were recorded using a Bruker AM250 pulsed Fourier transform instrument, infrared spectra were recorded on a Matteson Polaris FT-IR spectrometer as Nujol mulls between KBr plates. Melting points were measured in sealed tubes with an electrothermal melting point apparatus and are uncorrected. Microanalyses were carried out by the University College London service. Electron microscopy and elemental detection by analytical X-ray methods (EDAX) were carried out with a JEOL JS35CM scanning electron microscope; only qualitative results were obtained due to the lack of a suitable calibrant for InS and availability of suitable background correction in the instrument.

The X-ray powder diffraction patterns were measured using a thin-film analyzer on Siemens D5000 diffractometer using Cu Kα radiation of wavelength 1.5418 Å and a LiF monochromator. The sample was mounted at 1° and scanned from 10 to 90° in steps size of 0.02° with a count time of 12 s.

Single-Crystal X-ray Diffraction Study. Measurements were made on a sample mounted in a glass capillary with an Enraf-Nonius CAD4 diffractometer operating in the $\varpi/2\theta$ scan mode with graphite-monochromated Mo Kα radiation as described previously.[31] The structures were solved via standard heavy-atom procedures and refined by using full-matrix least-squares methods[32] with scattering factors calculated by using the data from ref 33. All non-hydrogen atoms were refined with anisotropic displacement factors; hydrogen atoms were identified in difference maps and included with isotropic displacement factors. Crystal data and the details of the intensity measurements and refinement are given in Table 2; atomic coordinates and equivalent isotropic displacement parameters are reported in Table 3. Tables of H atom coordinates, all bond lengths and angles, and anisotropic displacement factor coefficients are included in the supplementary material.

Deposition of Thin Films. Thin films of InS and GaS were grown on GaAs (100) by MOCVD. The experiments were carried out in a cold wall low-pressure MOCVD reactor described previously.[34] The reactor consists of a furnace for heating the precursor, a quartz halogen lamp to heat a graphite susceptor, a thermocouple to monitor the temperature of the susceptor, and a high-vacuum pump (Edward Model E2M5) to maintain the pressure close to 10^{-2} Torr in the system during growth experiments.

Results and Discussion

The compounds of stoichiometry $R_2MS_2CNEt_2$ (R = Me, Et or Np; M = In or Ga) were prepared by metathetical or redistribution methods as described in the Experimental Section. All the compounds are air sensitive. The indium compounds are white crystalline solids with well-defined melting points, soluble in most organic solvents, and can be recrystallized from petroleum spirits (60−80 °C) or pentane. The gallium compounds are transparent viscous liquids. Repeated attempts to crystallize these compounds from a variety of solvents at low temperature were unsuccessful. The gallium compounds seem to be less stable than the indium analogues and decompose over a short period of time, becoming yellowish in color.

X-ray Single-Crystal Structures of $Me_2InS_2CNEt_2$ (1) and $Et_2InS_2CNEt_2$ (2). The structures of compounds **1** and **2** were determined from single crystals by X-ray methods and are shown in Figures 1 and 2. Selected bond lengths and angles are summarized in Table 4. The structure of compound **1** contains two independent molecules of [$Me_2InS_2CNEt_2$] in the unit cell (Figure 3). The coordination is a distorted tetrahedron (InS_2C_2) with an expanded C(1)−In−C(2) bond angle (137.50(2)°), the sulfurs S(1)−In−S(2) subtend a much narrower angle (68.77(3)°). A similar S−In−S angle (69.40(7)°) was observed in tris(diethyldithiocar-

(31) Jones, R. A.; Hursthouse, M. B.; Malik, K. M.; Wilkinson, G. *J. Am. Chem. Soc.* **1979**, *101*, 4128.
(32) Sheldrick, G. M. SHELX 76, Program for Crystal Structure Determination; University of Cambridge: Cambridge, U.K., 1979.
(33) *International Tables for X-ray Crystallography*; Kynoch Press: Birmingham, U.K., 1974; Vol. 4.
(34) Malik, M. A.; O'Brien, P. *Adv. Mater. Opt. Electron.* **1994**, *3*, 171.

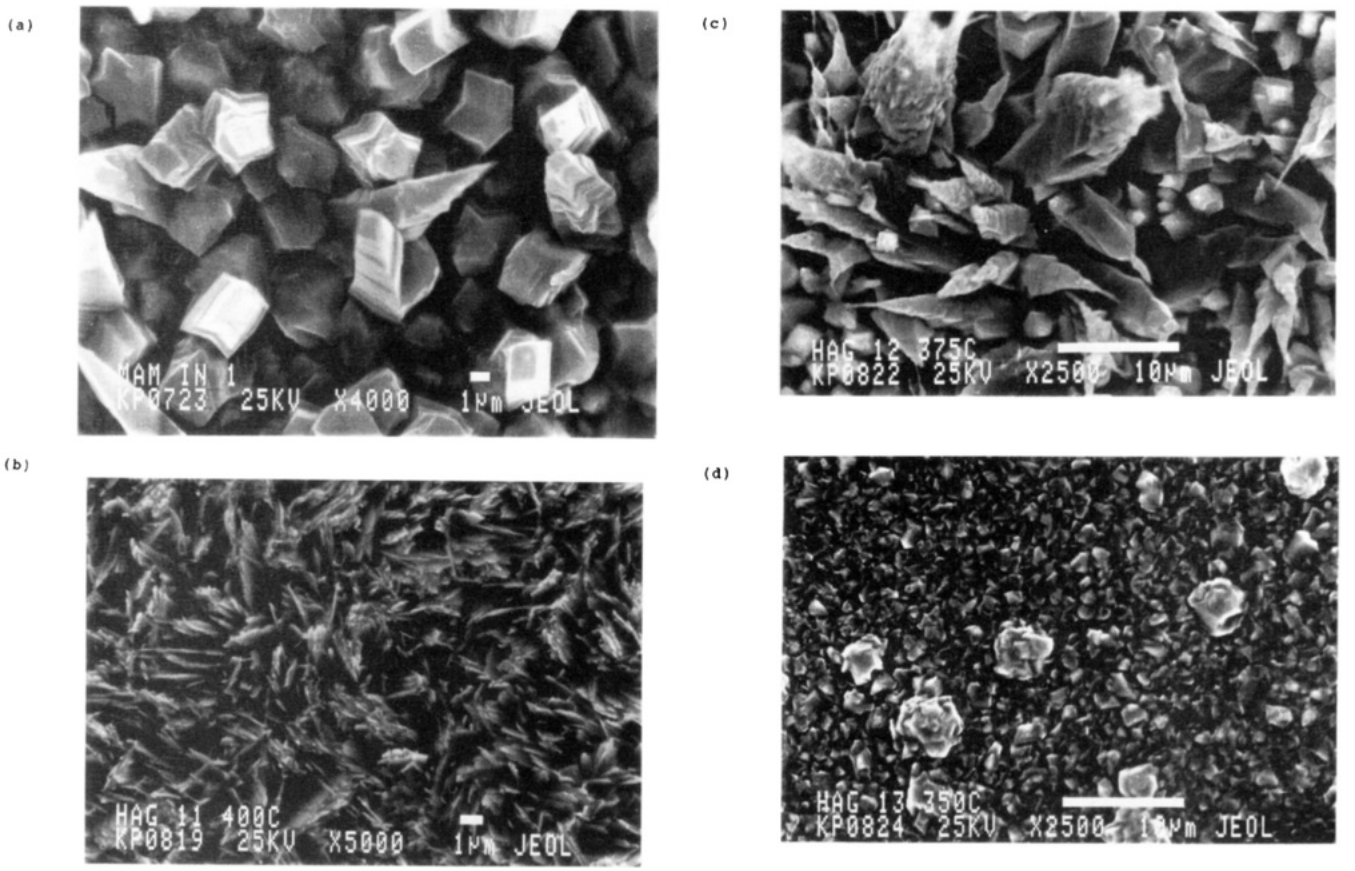

Figure 3. Electron micrographs of InS grown from $Me_2InS_2CNEt_2$, on GaAs(100) at (a) 425, (b) 400, (c) 375, and (d) 350 °C for 1 h.

Table 5. Growth and X-ray Powder Diffraction Results

compound	film	growth temp (°C)	precursor temp (°C)	phase	comments
1	InS	425	110	InS + In_6S_7	thick, black, crystalline film
	InS	400	110	InS + In_6S_7	thick, black, even coating
	InS	375	110	In_6S_7	dark gray, even film, more S present
	InS	350	110	In_6S_7	thin, gray, even film; further increase in S
	InS	325	110	β-In_2S_3	thinner, light gray, even film
2	InS	400	80	β-In_2S_3	thick, black, crystalline film
	InS	375	80	β-In_2S_3	black, even, crystalline film
	InS	350	80	β-In_2S_2	thin black film
3	InS	400	25	In_6S_7	thick, black, crystalline film
	InS	375	25	In_6S_7	thinner, black, even film
	InS	350	25		very little growth

bamato)indium(III),[30] which is presumably a result of the constraint imposed by chelation of the dithiocarbamato group. As is usual in such compounds, one of the two sulfurs attached to indium has a longer In−S separation than the other (In−S(1) = 2.67 Å, In−S(2) = 2.56 Å). The difference in bond distances observed for the two In−S contacts in structure **1** is larger than in other compounds containing similar ligands such as $In(S_2CNEt)_3$ (2.60 and 2.58 Å),[30] $In[S_2P(OEt)_2]_3$ (2.58 and 2.63 Å),[35] and In(dithiolene)$_3$ (2.59 and 2.63 Å).[36] The In−C bond lengths are slightly shorter (2.13−2.14 Å) than those reported previously for adducts such as $Me_3InN(^iPrCH_2)_3$ (2.15−2.19 Å[37]) and a range of adduct of trimethylindium with multidentate amines (2.22−2.25 Å[38]).

The structure of compound **2** is similar to that of **1** (see Figures 1 and 2 and Tables 2 and 4). The only major difference is that compound **2** contains a single monomer in the asymmetric unit instead of the two observed in **1**.

Spectroscopic Studies. Infrared spectra show clear bands for M−C, C−S, and C−N stretches. A considerable increase in stretching frequency is observed from indium to gallium as expected. ^{1}H NMR spectra of compounds **1** and **4** show a singlet at high field for two equivalent methyl (Me_2M) protons and a triplet and quartet for *N*-ethyl groups. Compounds **2** and **5** give a quartet and triplet for the equivalent ethyl groups Et_2M and show only a slight change in chemical shifts (see Experimental Section). Compounds **3** and **6** give two singlets for the equivalent neopentyl groups. For **3**, the lower field singlet is assigned to the methylene ($-CH_2M$) protons and the higher field singlet for the methyl protons ($CH_3)_3CCH_2M$. This situation is reversed for **6**. In summary, a considerable difference in the chemical shift is noticed for metal−methylene protons, In−

(35) Coggan, P.; Lebbeda, J. D.; McPhail, A. T.; Palmer, R. A. *J. Chem. Soc., Chem. Commun.* **1970**, 78.
(36) Einstein, F. W. B.; Jones, R. D. G. *J. Chem. Soc. A* **1971**, 2762.
(37) Bradley, D. C.; Frigo, D. M.; Harding, I. S.; Hursthouse, M. B.; Motevalli, M. *J. Chem. Soc., Chem. Commun.* **1992**, 577.
(38) Bradley, D. C.; Dawes, H.; Frigo, D. M.; Hursthouse, M. B. *J. Organomet. Chem.* **1987**, *325*, 55.

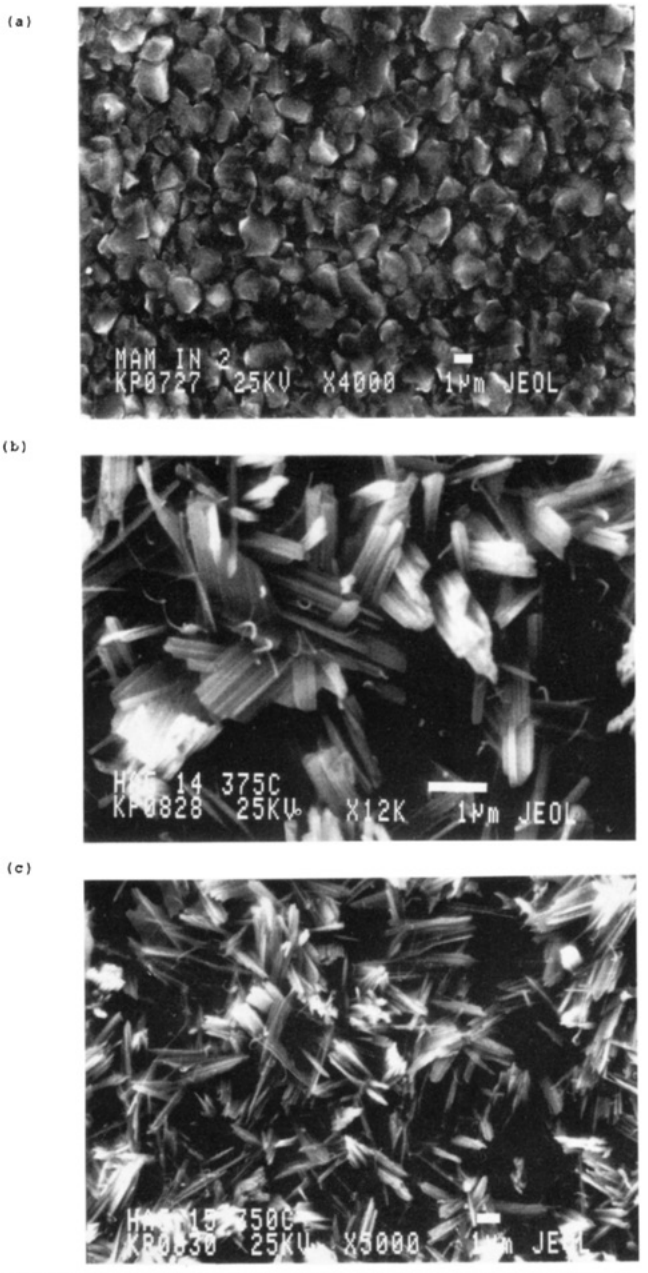

Figure 4. Electron micrographs of InS grown from $Et_2InS_2CNEt_2$, on GaAs(100) at (a) 400, (b) 375, and (c) 350 °C for 1 h.

CH_2– (1.48 ppm) and Ga–CH_2– (1.20 ppm) whereas the other signals show similar shifts.

^{13}C NMR spectra of compounds **1** and **4** had four signals, **2** and **5** had five signals, and **3** and **6** give six signals. Each show that both alkyl groups attached with metal are equivalent. The chemical shifts of methyl carbons show a significant change from indium (Me–In = −3.24 ppm) to gallium (Me–Ga = −0.86 ppm), whereas the other signals for N–Et protons show similar frequencies as expected. Other than the Me–In resonance, which appears at much higher field than Me–Ga, all other signals in indium compounds are at lower field than corresponding gallium compounds, the largest difference is shown by $-CH_2M$ carbons (see Experimental Section).

The mass spectra of all compounds show a molecular ion peak at the molecular mass of the compound minus the mass of one alkyl group, e.g., $MeInS_2CNEt_2$ for **1**. In the spectra of all compounds, the molecular ion peak

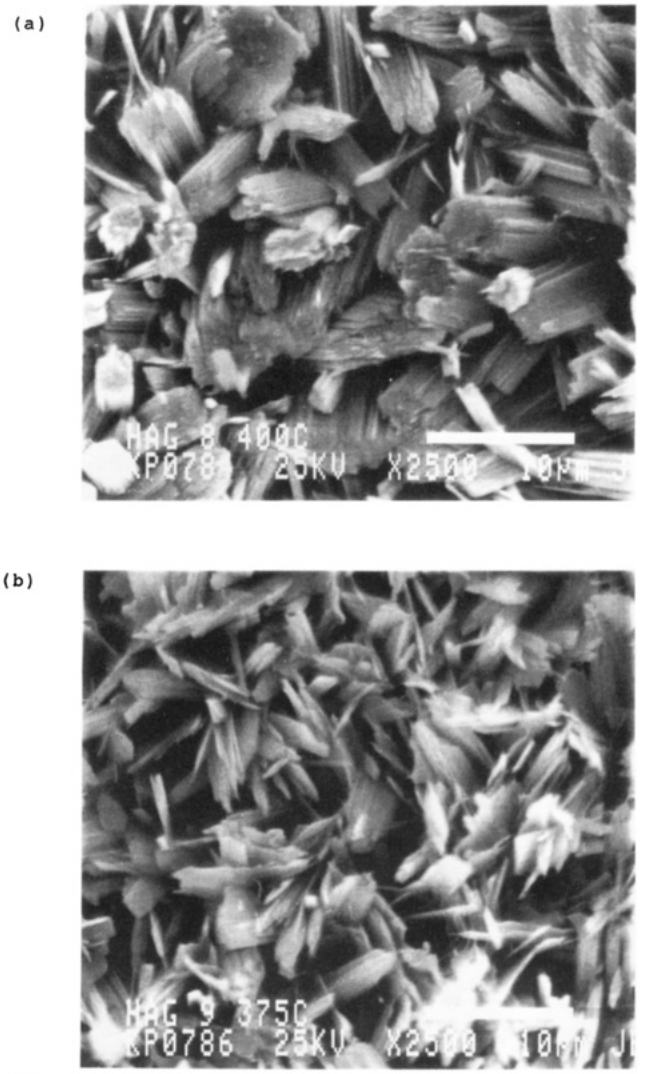

Figure 5. Electron micrographs of InS grown from $Np_2InS_2CNEt_2$, on GaAs(100) at (a) 400 and (b) 375 °C for 1 h.

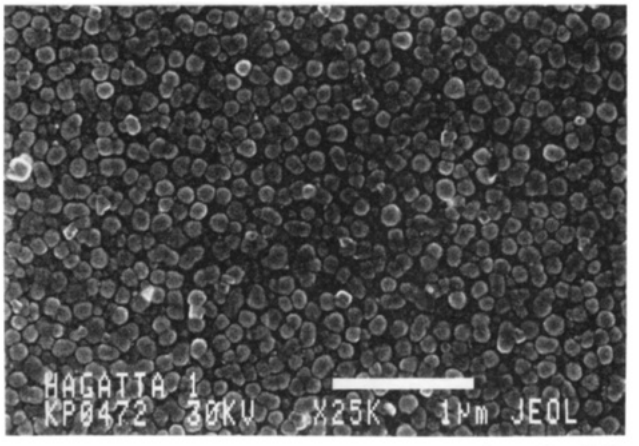

Figure 6. Electron micrograph of GaS grown from $Me_2GaS_2CNEt_2$, on GaAs(100) at 400 °C.

is also the base peak. The base peak suggests the monomer species are fairly stable as confirmed by the X-ray crystal structure of compound **1**. Other common fragments observed are $SCNEt_2$, SCNEt, $(EtN)_2$, HNEt, and NEt_2.

MOCVD Growth. As has been pointed out in the introduction there have been relatively few studies on the growth of III/VI materials as thin films, the choice of substrates for these materials is somewhat problem-

Table 6. X-ray Results for Thin Films Deposited from the Methyl (1) or Neopentyl (3) Precursors

ASTMS		ASTMS		methyl precursor (1)				neopentyl precursor (3)	
InS (*hkl*)	*I* (%)	In_6S_7 (*hkl*)	*I* (%)	350 °C (I%)	375 °C (I%)	400 °C (I%)	425 °C (I%)	375 °C (I%)	400 °C (I%)
1.92 (015)	10			1.94 (100)	1.94 (100)	1.94 (100)	1.94 (100)	1.94 (14)	1.94 (72)
1.97 (114)	66					1.97 (7)	1.96 (8)		
2.27 (113)	25							2.27 (41)	2.27 (47)
									2.35 (40)
							2.48 (10)	2.48 (46)	2.48 (42)
				2.57 (16)	2.55 (20)	2.57 (16)	2.57 (18)	2.57 (60)	2.57 (73)
2.66 (004)	60			2.65 (9)		2.65 (8)	2.65 (6)	2.65 (58)	2.65 (60)
2.77 (013)	4	2.78 (206)	30	2.75 (20)		2.75 (22)	2.75 (18)	2.75 (72)	2.75 (83)
		2.82 (304)	65	2.81 (15)		2.81 (16)		2.82 (70)	2.82 (71)
									2.90 (59)
2.95 (110)	100	2.95 (106)	25	2.95(11)		2.95 (28)	2.95 (25)		2.95 (62)
		3.00 (301)	95						
		3.19 (113)	90	3.18 (28)	3.16 (25)	3.18 (22)	3.18 (22)	3.19 (91)	3.19 (100)
							3.24 (33)	3.24 (100)	3.24 (80)
		3.39 (104)	65	3.38 (29)		3.37 (22)	3.38 (22)	3.38 (76)	3.38 (77)
3.41 (012)	70	3.43 (202)	55	3.42 (33)	3.40 (25)	3.42 (40)	3.43 (62)	3.43 (81)	3.43 (81)
		3.53 (105)	95	3.54 (38)	3.51 (33)	3.54 (46)	3.54 (73)	3.53 (79)	3.54 (74)
3.70 (101)	50					3.69 (20)	3.69 (40)		
		3.79 (011)	35	3.78 (70)	3.75 (73)	3.78 (68)	3.79 (55)	3.79 (86)	3.79 (79)
4.10 (011)	25	3.90 (201)	8						

atic. Substrates which have been used include Si(111) or quartz[11] (In_6S_7 and β-In_2S_3), GaAs(100) or Si(100) (InSe or In_2Se_3),[9] Si(100) or p-type Si(100)[16] (InS) and KBr or n- or p-type GaAs(100) (cubic GaS).[10] Few of these substrates are lattice matched, in the present work growth has generally been carried out using GaAs-(100) as in several of these studies.[9,10] Some experiments, especially in attempts to deposit GaS, were carried out using glass microscope slides or KBr plates; good-quality films were not obtained on these substrates.

Indium Sulfide. Indium sulfide has been grown using the methylindium **(1)**, ethylindium **(2)**, and neopentylindium **(3)** compounds at temperatures from 425 to 325 °C on GaAs(100) substrates (Table 5). Good-quality films were grown at all temperatures; the three compounds proved effective as precursors. Compound **1** proved to be the best precursor in terms of the overall quality and rate of growth of the films deposited. Reasonably thick films were deposited at 325 °C using **1**, whereas the other two precursors gave little or no deposition below 350 °C. The precursors **1** and **3** gave black crystalline films with ca. 4–5 μm crystallites, **2** gave comparatively thinner films with a crystalline size of ca. 2–3 μm. Precursor **2** gave paler colored indium sulfide films. At higher temperatures (425 °C), the physical appearance of the crystallites deposited from the methylindium compound **1** appeared rectangular in shape, but at lower temperatures irregular long flakes were found. Electron micrographs of films grown from ethyl and neopentylindium compounds show large rod-like, randomly orientated crystallites at all temperatures, although the size of the crystallites vary with temperature. Typical electron micrographs showing crystallites of indium sulfide deposited from precursors **1**–**3** at various temperatures are shown in Figures 3–6. These results can be compared to those of Nomura, who deposited indium sulfide films[11] using precursors of the type ^{n}BuIn(S^iPr)$_2$. The films were amorphous when grown at ca. 300 °C and crystalline at ca. 400 °C.

The EDAX profiles of all the films show the presence of indium and sulfur. The EDAX results are not quantitative, but the intensity of the sulfur peaks gives a reasonable indication of the sulfur content in an individual film. For example, a more intense sulfur peak is observed in the film grown from compound **2**, an In_2S_3 phase as compared to In_6S_7 phases in the films grown from compound **3**. The results of the growth experiments using compounds **1**–**3** are summarized in Table 5.

Analysis of the powder diffraction patterns reveals the presence of a number of different phases in the indium sulfide films. This is especially true for the films deposited from the methylindium precursor **1** (Table 6, Figure 7). Powder diffraction patterns of the thin films grown using the methylindium compound **1** reflect the complexity observed in the electron micrographs Figure 3. At 425 and 400 °C there is an even distribution of orthorhombic InS[39] and monoclinic In_6S_7[39] phases, whereas at 375 and 350 °C, the In_6S_7 phase is dominant (ca. 75%). Growth at 325 °C resulted in the cubic β-In_2S_3 phase with some evidence for preferred orientation along the (113) plane. All the other phases tend to have preferred orientation along the (015) plane. In general the sulfur content of the layers increases at lower growth temperatures. Nomura et al.[11] had previously reported a similar observation using ^{n}BuIn(S^iPr)$_2$ and have suggested that at higher temperatures the decrease in sulfur content of the indium sulfide layers results from the premature release of a sulfur moiety from the precursor. We believe that the loss of sulfur by evaporation from the surface of the deposited layer may also be important. Compounds **1**–**3** are chelates which makes removal of a single sulfur substantially harder than the removal of a S^iPr ligand from ^{n}BuIn-(S^iPr)$_2$.

The powder diffraction patterns of the indium sulfide films grown from the ethyl indium compound **2** (Table 7, Figure 8) showed only one crystalline phase over the 400–350 °C temperature range and the morphology observed in the electron micrographs reflects this observation (Figure 4b,c) although at 400 °C the crystallinity may be better developed (Table 7). This is the sulfur-rich cubic β-In_2S_3[41] phase. The XRD patterns of the films deposited from the neopentyl indium compound **3** (Table 6, Figure 9) show two phases of indium sulfide, In_6S_7 at 400 °C and 375 °C with the presence of

(39) Duffin, W. J.; Hogg, J. H. C. *Acta Crystallogr.* **1966**, *20*, 566.
(40) Kabalkina, S. S.; Losev, V. G. *Solid State Commun.* **1982**, *44*, 1383.
(41) Hahn, V. H.; Klingler, W. *Z. Anorg. Chem.* **1949**, *260*, 97.

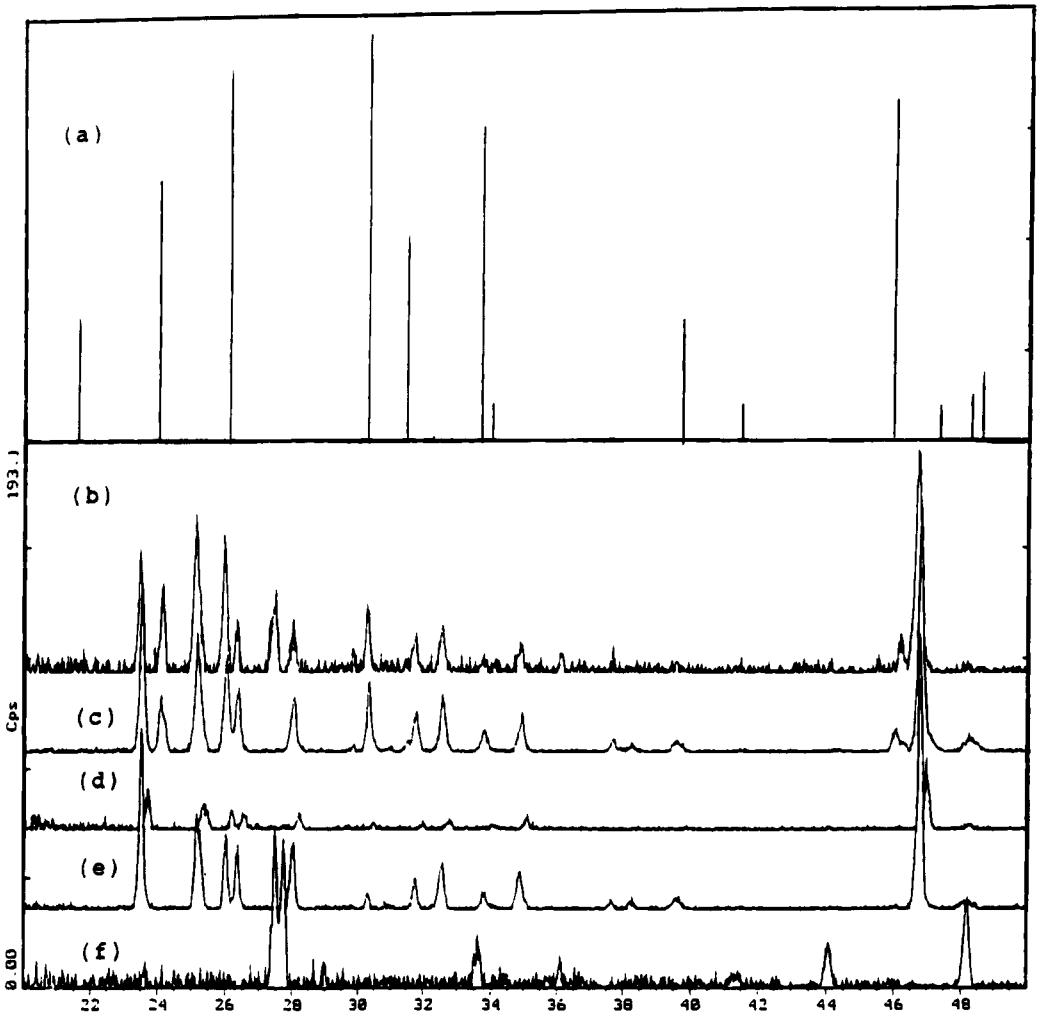

Figure 7. (a) Standard X-ray powder diffraction pattern of InS. Pattern for indium sulfide grown from $Me_2InS_2CNEt_2$ at (b) 425 °C, (c) 400 °C, (d) 375 °C, (e) 350 °C, (f) 325 °C showing different phases.

Table 7. X-ray Results for Thin Films Grown from the Ethyl (2) Precursor (I%)

d/Å (*hkl*)	ASTMS (I%)	350 °C	375 °C	400 °C
1.64 (533)				10
1.7 (620)	25			
1.81 (531)	35			
1.89 (440)	100	37	42	53
1.98 (520)	18			
2.07 (511)	75	20	23	30
2.19 (422)	35	3	5	10
2.47 (331)	18	2	2	8
2.53 (411)	18			
2.60 (410)	8			
2.68 (400)	50	28	26	30
3.10 (222)	25	4	5	20
3.24 (311)	65	100	100	100
3.56 (300)	8			
3.75 (220)	35	12	26	36

some of the β-In_2S_3 phase indicated by a peak at 3.24 Å. The growth is similar to that reported recently[9] for InSe grown from the $Me_2InSePh$ precursor at 365 °C. The films grown from the ethyl precursor **2** appear to have particularly intense peaks consistent with orientation of growth in the (311) plane for all films at all temperatures.

Gallium Sulfide. The deposition of gallium sulfide from the diethyldithiocarbamates of gallium was in general less successful, and only some preliminary observations are reported. Thin, specular, adherent, apparently crystalline films (by electron microscopy) of gallium sulfide were grown on GaAs(100) using $Me_2GaS_2CNEt_2$ (**4**). Gallium sulfide films deposited at 400 °C appeared gold in color. The EDAX profile of the film deposited from compound **4** showed low-intensity peaks for both gallium and sulfur. None of the films of gallium sulfide gave powder diffraction patterns; the films may simply be too thin for patterns to be detected in our equipment as the films appear crystalline from the electron micrographs. An electron micrograph of gallium sulfide grown at 400 °C (Figure 6) showed smooth films with random growth of crystallites of ca. 100 nm.

The other two gallium precursors, compounds **5** and **6**, gave little or no deposition of gallium sulfide (450–300 °C); only gallium could be detected by EDAX.

Conclusions

Preliminary growth work shows that dialkyldithiocarbamatoindium(III) complexes are useful single-molecule precursors for the growth of indium sulfide thin films. XRD results showed the presence of InS, In_6S_7, and β-In_2S_3 depending upon the growth temperature and the precursor used. The fastest growth rates were achieved with the methyl precursor **1**. The ethyl precursor **2** differed from the other two compounds in that a single phase, cubic β-In_2S_3, was deposited over the entire temperature range studied. Only the ethyl precursor contains β-hydrogen atoms, and the ready elimination of the alkyl fragment may influence the films composition in a number of ways, including by

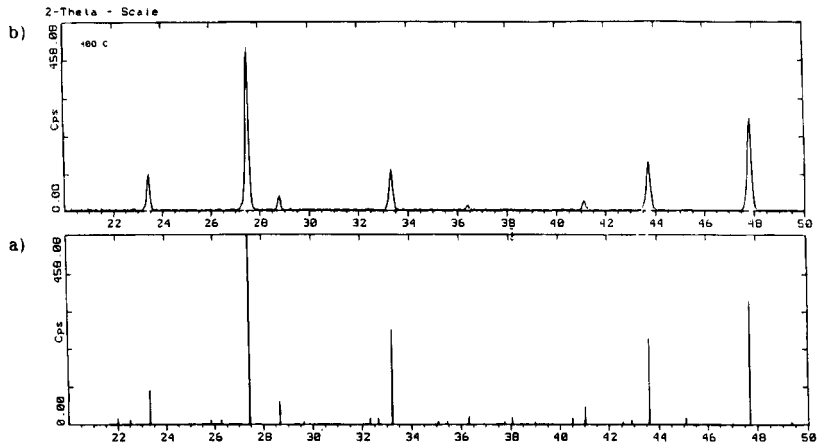

Figure 8. (a) Standard X-ray powder diffraction pattern of β-In_2S_3. Pattern for indium sulfide grown from $Et_2InS_2CNEt_2$ at (b) 400 °C.

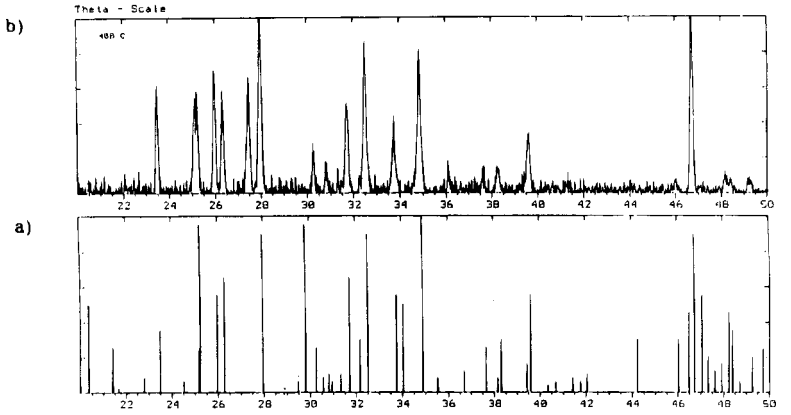

Figure 9. (a) Standard X-ray powder diffraction pattern of In_6S_7. Pattern for indium sulfide grown from $Np_2InS_2CNEt_2$ at (b) 400 °C.

affecting the amount of carbon incorporation. Only very thin films of gallium sulfide were grown and only from the dimethyldiethyldithiocarbamatogallium(III) (**4**); the other gallium precursors gave no deposition of gallium sulfide. These growth studies indicate also that the quality and nature of the films deposited can be affected by varying the alkyl groups attached to the metal. In the case of indium, the phase deposited depends on both the temperature used and the precursor chosen.

Barron suggests that the shape of the precursor will determine the phase of the film deposited; hence the dimeric precursor $[(^tBu)_2In(S^tBu)]_2$[16] is suggested to deposit tetragonal[40] InS *because* of the structure of the In_2S_2 core in the precursor. However the deposition of the high-temperature form of zinc sulfide[42] (the cubic phase, zinc blende) at low temperatures, from the bisdiethyldithiocarbamate, has been attributed to the control of phase by the delivery of sulfur to the material, i.e., an effect of sulfur fugacity on the phase deposited.[43] Our results, especially the fact that several phases are deposited using compound **1**, suggest that many factors control the phase deposited in an MOCVD experiment, any simple explanation based on the shape of precursor is probably only part of a complicated mechanistic story. A suggestion which is supported by the recent observation that the pyrolysis of solid $[Zn(SEt)Et]_{10}$ leads to cubic ZnS even though the structure of the precursor complex closely resembles that of wurtzite the hexagonal modification of ZnS.[44] Another factor which may affect the phase deposited is carbon incorporation, especially as the ethyl precursor deposits a single phase the only compound in the series to which β-elimination is positive. Studies of carbon incorporation into these films are in hand.

Acknowledgment. The present work has been supported by EPSRC grants to Dr. P. O'Brien and a SERC Quota Studentship to SH from the I.R.C. for semiconducting materials, Imperial College, London. We thank Mr. Keith Pell of the QMW Electron Microscopy Unit for SEM and Mr. Peter Cook for mass spectroscopy.

Supplementary Material Available: Tables of H atom coordinates, bond lengths and angles, and anisotropic displacement factor coefficients (13 pages); list of observed and calculated structure factor amplitudes (16 pages). Ordering information is given on any current masthead page.

CM940496H

(42) Pike, R. D.; Cui, H.; Kershaw, R.; Dwight, K.; Wold, A.; Blanton, T. N.; Wernberg, A. A.; Gysling, H. J. *Thin Solid Films* **1993**, *224*, 221.

(43) Scott, S. D.; Barnes, H. L. *Geochim. Cosmochim. Acta* **1972**, *36*, 1275.

(44) Zeng, D.; Hampden-Smith, M. J.; Duesler, E. N. *Inorg. Chem.* **1993**, *33*, 5376.